A centrosome asymmetry switch in fly neural stem cells

Emmanuel Gallaud[1, *], Anjana Ramdas Nair[1, 3, *], Arnaud Monnard[1,2], Priyanka Singh[1,4], Tri Thanh Pham[1,2], David Salvador Garcia[1,5], Alexia Ferrand[1] & Clemens Cabernard[2, #]

[1] Biozentrum, University of Basel
Klingelbergstrasse 50-70
CH-4056 Basel, Switzerland

[2] Department of Biology, University of Washington
24 Kincaid Hall
Seattle, WA 98105, USA

[3] Present address:
NYU Abu Dhabi, Saadiyat Campus
Abu Dhabi, United Arab Emirates

[4] Present address:
Department of Bioscience & Bioengineering, Indian Institute of Technology Jodhpur
NH 65, Nagour Road, Karwar, Jodhpur District,
Rajasthan, India 342037.

[5] Present address:
Division of Cell Biology, MRC Laboratory of Molecular Biology
Francis Crick Avenue
Cambridge CB2 0QH, UK.

* These authors contributed equally

[#] Correspondence to: ccabern@uw.edu

Centrosomes, the main microtubule organizing centers (MTOCs) of metazoan cells, contain an older 'mother' and a younger 'daughter' centriole. Stem cells either inherit the mother or daughter centriole, providing a mechanism for biased delivery of cell fate determinants. However, the molecular mechanisms regulating centrosome asymmetry and biased centrosome segregation are unclear. Using 3D-Structured Illumination Microscopy (3D-SIM), we here identify a centrosome asymmetry switch in fly neural stem cells. We show that the mitotic kinase Polo and its substrate, the centriolar protein Centrobin (Cnb), relocalize from the mother to the forming daughter centriole in mitosis. Polo's relocalization depends on both Centrobin and Wdr62, and compromising the switch perturbs biased interphase MTOC activity. We propose that this asymmetry switch is necessary to form molecular and functional asymmetric centrosomes and the neuroblast specific retention of the daughter centriole-containing centrosome. The centrosome asymmetry switch might also explain the differences in centrosome inheritance across stem cell systems.

Introduction

Centrosomes consist of a pair of centrioles, embedded in structured layers of pericentriolar material (PCM)[1]. A single 'daughter' centriole is formed around a central cartwheel and at right angles to the existing older 'mother' centriole [2,3]. Based on this replication cycle, centrioles - and thereby centrosomes - are intrinsically asymmetric. Stem cells have been observed to inherit either the mother or daughter centriole-containing centrosome (mother and daughter centrosome, hereafter). For instance, vertebrate neural stem cells or *Drosophila* male germline stem cells obtain the older mother centrosome, raising the possibility that it contains factors necessary to maintain stemness [4,5]. However, *Drosophila* female germline or neural stem cells, called neuroblasts, inherit the daughter centrosome [6-8]. The role of centrosomal age in determining cell fate and the difference in centriole inheritance among different stem cell types is unclear.

Drosophila neuroblasts represent an ideal genetically tractable system to investigate centrosome asymmetry [9]. Neuroblast centrosomes are highly asymmetric in interphase; one centrosome is forming an active MTOC, whereas its sibling remains inactive until entry into mitosis [7,10,11]. The active interphase MTOC contains the daughter centriole, identifiable with the orthologue of the human daughter centriole-specific protein Cnb (Cnb^{+}) [6]. This biased MTOC activity is regulated by the mitotic kinase Polo (Plk1 in vertebrates). Polo phosphorylates Cnb, necessary to maintain an active MTOC, tethering the daughter centriole-containing centrosome to the apical interphase cortex. Cortical association ensures that the daughter centrosome is inherited by the self-renewing neuroblast [6,12] (and Figure S1A). Polo localization on the apical centrosome is maintained by the microcephaly associated protein Wdr62 [13]. The mother centrosome, separating from the daughter centrosome in interphase, downregulates Polo and MTOC activity through Pericentrin (PCNT)-like protein (Plp) and Bld10 (Cep135 in vertebrates) [14,15]. The lack of MTOC activity prevents the mother centrosome from engaging with the apical cell cortex; it randomly migrates through the cytoplasm until centrosome maturation in prophase establishes a second MTOC near the basal cortex, ensuring its segregation into the differentiating ganglion mother cell (GMC). Later in mitosis, the mother centrosome also accumulates Cnb [7,10,11,14] (and Figure S1A). Although several centrosomal proteins have been described to be enriched on either the mother or daughter centriole

containing centrosome [6,13,16], it is unknown when and how centrioles acquire a unique molecular identity. Here, we describe a novel centrosome asymmetry switch manifested in the dynamic transitioning of both Polo and Cnb from the mother to the daughter centriole. This switch, occurring in mitosis, is necessary for subsequent asymmetric MTOC activity, centrosome positioning and biased centrosome segregation.

Results

We used 3D-Structured Illumination Microscopy (3D-SIM), which has approximately twice the spatial resolution of standard confocal microscopy, to investigate the centriole duplication cycle and to determine the onset of molecular centrosome asymmetry in third instar neuroblasts (Figure 1A). In vertebrate cells, centriole duplication occurs in S-phase (reviewed in [3,17,18]) but it is unclear whether this is also the case in *Drosophila* neural stem cells. Using 3D-SIM on fixed larval neuroblasts, we found that Sas-6 and Ana-2 were localized to the centriolar cartwheel whereas Ana-1, Bld10 and Asl form ring-like structures abutting the centriolar wall (Figure S2A-C).

We used Sas-6 and Asl to determine the onset of cartwheel duplication and centriolar wall maturation during the neuroblast cell cycle. Cell cycle stages were determined based on the organization of the microtubule network (Figure S1B). Apical and basal interphase neuroblast centrosomes contained two Sas-6^+ cartwheels but only one Asl^+ centriole. From prometaphase onwards, Asl gradually appeared around the second cartwheel to form a pair of fully formed centrioles. A similar sequential loading of proteins was observed in S2-cells [19]. In telophase, centrioles appeared to lose their orthogonal conformation, possibly because of disengagement. In late telophase, cartwheels duplicated, manifested in the appearance of a third Sas-6 positive cartwheel (Figure 1B). Based on these data we conclude that centriolar cartwheels are duplicated in early interphase. The localization of Asl to the centriolar wall starts in early mitosis but is not completed before the end of mitosis.

Centrosome asymmetry is detectable in interphase neuroblasts but when the centrosome, inherited by the neuroblast, acquires its unique molecular signature is unclear (Figure 2A, C). For instance, Cnb is localized to the single apical centriole in interphase neuroblasts [6]. Since this centriole forms the template

for the formation of the daughter centriole, Cnb must either switch its localization to the newly formed daughter centriole in mitosis or – in contrast to a previous report [6] – Cnb is localized to the old mother centriole that is being inherited by the self-renewing neuroblast. To resolve this issue, we analyzed the localization of YFP::Cnb [6] with 3D-SIM throughout mitosis. As expected, YFP::Cnb was localized with Asl on the active, apical centrosome in interphase neuroblasts but absent on the basal interphase centrosome (Figure 2B, D and Figure S2D). Also, most apical prophase centrosomes contained a single Cnb^{+} centriole (dark blue arrowheads in Figure 2B); the basal prophase centrosomes were mostly Cnb^{-}. To our surprise, we also found apical - but never basal - prophase and prometaphase centrosomes where Cnb was localized on both centrioles (green arrowheads in Figure 2B). However, from metaphase onwards Cnb was predominantly localized on one centriole only (brown arrowheads in Figure 2B). On the basal centrosome, Cnb appeared in prophase but was always localized to one centriole only in all subsequent mitotic stages (Figure 2D and Figure S2D).

To better understand Cnb relocalization dynamics, we correlated centriolar age with Cnb localization in more detail. To this end, we first calculated the Asl intensity ratio between both centrioles (see methods) from apical and basal centrosomes containing Cnb only on one of the two centrioles (Asl intensity ratio of Cnb^{+}/Cnb^{-} from prometaphase until telophase). We detected an inherent asymmetry in Asl intensity, consistent with the sequential loading of Asl onto the forming daughter centriole: for all centrosomes containing one Cnb^{+} and one Cnb^{-} centriole, the Cnb^{+} centriole always contained less Asl (Figure 2E). In addition, this Asl intensity correlated well with the morphology of early mitotic centrioles; the fully formed centriole always contained more Asl. Thus, we used Asl as a centriolar age marker [19,20] and reanalyzed all mitotic stages for Cnb localization on the apical centrosome, specifically focusing on stages where Cnb appeared on both centrioles. We found that in prophase – when Cnb was detectable on both centrioles – Cnb was predominantly associated with the centriole containing more Asl (the mother centriole) before switching to the centriole containing less Asl (the daughter centriole) during prometaphase (green arrowhead in Figure 2B). Cnb was sometimes visible before Asl was robustly recruited to the daughter centriole (green arrowheads in third column of Figure 2B). From metaphase until mitosis exit, Cnb was

strongly enriched or exclusively present on the daughter centriole (Figure 2F, G and Figure S3A-C). Interestingly, Cnb localization dynamics differed between the apical and basal centrosome; the basal centrosome contained a single Asl^{+}, Cnb^{-} centriole in interphase and Cnb appeared on the forming centriole in prophase (Figure 2D).

From these data, we can conclude the following: (1) centrosome asymmetry is tightly coupled to the centriole duplication and maturation cycle. (2) On the apical centrosome, Cnb is switching its localization from the mother to the daughter centriole during prophase to prometaphase. (3) On the basal centrosome, however, Cnb seems to be recruited directly to the youngest centriole. These observations suggest that apical neuroblast centrosomes undergo a spatiotemporally controlled 'asymmetry switch' in mitosis.

To test whether this asymmetry switch also applies to other centrosomal proteins, we analyzed the localization of Polo (Polo::GFP) and Plp (Plp::EGFP) throughout mitosis; both Polo and Plp were GFP-tagged at the endogenous locus ([21] and methods). In early prophase neuroblasts and on both centrosomes, Polo was localized on the existing centriole (Figure 3A, B & [13]). Subsequently, Polo intensity increased on the forming daughter centriole on both centrosomes and its asymmetric localization peaked in metaphase/anaphase. Interestingly, the apical centrosome showed a less pronounced asymmetric distribution in prometaphase compared to the basal centrosome, which could reflect differences in the relocalization mechanism (Figure 3A-C).

In contrast to Polo and Cnb, Plp predominantly remained localized on the mother centriole on both centrosomes, although it increased also on the daughter centriole in late mitosis (Figure S4A-C). Co-imaging Polo together with Plp, and Cnb with Plp showed that Plp separated from Polo and Cnb in metaphase and anaphase (Figure 3D, E). These data suggest that similar to Cnb, Polo switches its localization from the mother to the daughter centriole, whereas Plp remains localized on the mother centriole. However, in contrast to Cnb, Polo is switching its localization on both centrosomes.

Next, we sought to determine the molecular mechanisms underlying this centrosome asymmetry switch. We analyzed Asl, Polo and Plp localization in neuroblasts depleted for Cnb (*cnb* RNAi) and Wdr62. Wdr62 is implicated in primary microcephaly [22-24], and both Cnb and Wdr62 are necessary for the

153 establishment and maintenance of centrosome asymmetry by regulating Polo's and Plp's centrosomal
154 localization in interphase neuroblasts [12,13]. Lack of Cnb or Wdr62 did not compromise the gradual loading
155 of Asl onto the newly formed centriole in mitotic neuroblasts (data not shown). However, in the absence of
156 Cnb and Wdr62, the asymmetric centriolar localization of Polo, especially in prometaphase to anaphase
157 neuroblasts, was significantly perturbed (Figure 4A-C). Lack of Cnb - but not Wdr62 - also compromised
158 Polo's asymmetric localization in telophase, suggesting a preferential requirement for Wdr62 in metaphase
159 and anaphase. Taken together, loss of *cnb* or *wdr62* significantly increased the number of centrosomes with
160 inverted Polo asymmetry ratios (wild type control: 8.6%; *cnb* RNAi: 40%; *wdr62*: 31.5%; Figure 4D, E).
161 Plp localization was still highly asymmetric in neuroblasts depleted for Cnb and Wdr62. However, Cnb
162 depletion decreased, and loss of Wdr62 further increased Plp's asymmetric localization (Figure S5A-D).
163 We conclude that in mitotic neuroblasts, Cnb has a minor role in promoting the asymmetric localization of
164 Plp, whereas Wdr62 could have a permissive role in Plp recruitment on the daughter centriole. Taken
165 together, these data suggest that both Cnb and Wdr62 are implicated in Polo's switch from the mother to
166 the daughter centriole.

167 Finally, we set out to investigate the consequences of the centrosome asymmetry switch by
168 preventing the transitioning of Cnb and Polo from the mother to the daughter centriole. Since our 3D-SIM
169 data showed Plp to be predominantly associated with the mother centriole, we reasoned that tethering Cnb
170 to the mother centriole with Plp's PACT domain [25] would compromise the establishment of a Cnb^- mother
171 and Cnb^+ daughter centriole. We speculated that Cnb's localization would remain enriched on the mother
172 or at least become near symmetrically localized between the mother and daughter centriole. Indeed, 3D-
173 SIM experiments revealed that YFP::Cnb::PACT [12] failed to properly transition from the mother to the
174 daughter centriole and predominantly remained associated with the mother centriole (Figure S6A, B).
175 Direct linking of Cnb to centrosomes using the PACT domain (YFP::Cnb::PACT) has also been shown to
176 convert the inactive mother interphase centrosome into an active MTOC, resulting in the presence of two
177 active interphase MTOCs [12] (Figure S6C & Movie 1, 2). This result suggested that disrupting the
178 centrosome asymmetry switch in mitosis impacts MTOC behavior in interphase.

To further test this, we developed a nanobody trapping experiment, using the anti-GFP single domain antibody fragment (vhhGFP4) [26,27] and the PACT domain of Plp [25] to trap GFP- or YFP-tagged proteins on the mother centriole (Figure S7A-C). We could recapitulate the interphase MTOC phenotype of YFP::Cnb::PACT by expressing PACT::vhhGFP4 in neuroblasts together with YFP::Cnb; almost 93% (n=69) showed two active interphase MTOCs (YFP::Cnb expression only: 0%; n = 16; Figure S7D, E & Movie 3). Conversely, trapping Asl::GFP with PACT::vhhGFP4 on the mother centriole did not cause a significant MTOC phenotype; 83% of neuroblasts showed normal divisions (n = 104; Figure S7F, G & Movie 4).

Co-expressing a GFP-tagged version of Polo – either a published GFP::Polo transgene [28] or our endogenously tagged CRISPR Polo::EGFP line – prevented the transitioning of Polo from the mother to the daughter centriole. 3D-SIM data revealed that Polo::EGFP was predominantly localized to the mother centriole in prophase and prometaphase. Subsequently, Polo::EGFP was either enriched on the mother or symmetrically localized from metaphase onwards (Figure 5A,B). This altered localization affected MTOC activity in third instar neuroblasts; similar to Cnb mislocalization, trapping Polo on the mother centriole induced the formation of two active interphase MTOCs (GFP::Polo transgene: 84%; n = 31. Polo::EGFP CRISPR line: 72%; n = 82) (Figure 5C-E, Figure S7H, I & Movie 5-7). Although cell cycle progression was not affected in these neuroblasts (Figure 5F), we measured a significant misorientation of the mitotic spindle in early metaphase. However, similar to *bld10*, displaying two active interphase MTOCs also [14], mitotic spindles realigned along the apical-basal polarity axis, ensuring normal asymmetric cell divisions (Figure 5G-J). We hypothesized that preventing the establishment of a clear Polo asymmetry in mitosis transforms the two centrosomes into apical-like interphase centrosomes. Indeed, 3D-SIM imaging revealed that both centrioles now contain high levels of centriolar, and diffuse PCM Polo levels as we recently described for the apical interphase wild type centrosome [13] (Figure 6K,L).

Discussion

Here, we have shown that in *Drosophila* neural stem cells, centrosomes undergo a previously undiscovered asymmetry switch by transferring centriolar proteins such as Cnb or Polo from the old mother to the young daughter centriole. This centrosome asymmetry switch is tightly linked to the centriole duplication cycle, coinciding with the completion of daughter centriole formation in mitosis. In prophase, Cnb and Polo colocalize on the existing mother centriole but as soon as the daughter centriolar wall appears in prometaphase, Cnb and Polo are exclusively (in the case of Cnb) or predominantly (in the case of Polo) localized on the daughter centriole. Interestingly, Cnb behaves differently on the basal centrosome since the existing mother centriole does not contain any Cnb, appearing only on the forming daughter centriole in prometaphase. Also, Plp remains predominantly associated with the mother centriole on both the apical and basal centrosome (Figure 6A, B). Mechanistically, this asymmetry switch could entail a direct translocation of Cnb and Polo from the mother to the daughter centriole. Alternatively, centriolar proteins could become up- or downregulated through exchanges with the PCM or cytoplasm. The asymmetry switch might also be regulated differently on the apical versus basal centrosome. Our data suggest that Polo's relocalization to the daughter centriole is regulated by both Cnb and Wdr62 since loss of either protein compromises the enrichment of Polo on the daughter centriole. However, Cnb's relocalization is independent of Polo; *polo* mutants still show mostly normal Cnb transfer to the daughter centriole (data not shown).

The centrosome asymmetry switch is important for interphase MTOC activity. Using our nanobody trapping experiment, we could efficiently compromise the transitioning of Polo and Cnb from the mother to the daughter centriole, with the consequence that both centrosomes retained MTOC activity in interphase. Although this experiment is performed in the presence of untagged Polo, which is not subject to direct nanobody trapping and cannot be visualized, the trapping of GFP-tagged Polo alone seems sufficient to disrupt the normal asymmetric distribution of Polo to compromise biased interphase MTOC activity. This result is also in agreement with *bld10* mutants which fail to downregulate Polo from the mother centriole, resulting in the formation of two active interphase MTOCs [14]. Loss of Wdr62 or Cnb also affects Polo's

mother – daughter transition. Yet, interphase centrosomes lose their activity in these mutants. *wdr62* mutants and *cnb* RNAi treated neuroblasts both show low Polo levels in interphase [13]. We thus propose that in addition to an asymmetric distribution, Polo levels must remain at a certain level to maintain interphase MTOC activity; high symmetric Polo results in two active interphase MTOCs whereas low symmetric Polo results in the formation of two inactive centrosomes.

Taken together, these results suggest that the centrosome asymmetry switch is necessary to establish two molecularly distinct centrioles, necessary for the biased MTOC activity in interphase (Figure 6A, B). Furthermore, the switch also provides a molecular explanation for why the daughter centriole-containing centrosome remains tethered to the apical neuroblast cortex and is being inherited by the self-renewed neuroblast. It remains to be tested why neuroblasts implemented such a robust machinery to asymmetrically segregate the daughter-containing centriole to the self-renewed neuroblast; more refined molecular and behavioral assays will be necessary to elucidate the developmental and post-developmental consequences of the centrosome asymmetry switch. The tools and findings reported here will be instrumental in targeted perturbations of the centrosome asymmetry switch with spatiotemporal precision in defined neuroblast lineages.

Finally, the occurrence of a centrosome asymmetry switch further raises the tantalizing possibility that centriolar proteins also transfer in other stem cells, potentially providing a mechanistic explanation for the differences in centriole inheritance across different stem cell systems.

References

1. Mennella, V. *et al.* Subdiffraction-resolution fluorescence microscopy reveals a domain of the centrosome critical for pericentriolar material organization. *Nat. Cell Biol.* **14,** 1159–1168 (2012).
2. Nigg, E. A. & Raff, J. W. Centrioles, Centrosomes, and Cilia in Health and Disease. *Cell* **139,** 663–678 (2009).
3. Conduit, P. T., Wainman, A. & Raff, J. W. Centrosome function and assembly in animal cells. *Nat. Rev. Mol. Cell Biol.* **16,** 611–624 (2015).
4. Wang, X. *et al.* Asymmetric centrosome inheritance maintains neural progenitors in the neocortex. *Nature* **461,** 947–955 (2009).
5. Yamashita, Y. M., Mahowald, A. P., Perlin, J. R. & Fuller, M. T. Asymmetric inheritance of mother versus daughter centrosome in stem cell division. *Science* **315,** 518–521 (2007).
6. Januschke, J., Llamazares, S., Reina, J. & Gonzalez, C. Drosophila neuroblasts retain the daughter centrosome. *Nat Commun* **2,** 243 (2011).
7. Conduit, P. T. & Raff, J. W. Cnn dynamics drive centrosome size asymmetry to ensure daughter centriole retention in Drosophila neuroblasts. *Curr. Biol.* **20,** 2187–2192 (2010).
8. Salzmann, V. *et al.* Centrosome-dependent asymmetric inheritance of the midbody ring in Drosophila germline stem cell division. **25,** 267–275 (2014).
9. Gallaud, E., Pham, T. & Cabernard, C. Drosophila melanogaster Neuroblasts: A Model for Asymmetric Stem Cell Divisions. *Results Probl Cell Differ* **61,** 183–210 (2017).
10. Rebollo, E. *et al.* Functionally unequal centrosomes drive spindle orientation in asymmetrically dividing Drosophila neural stem cells. *Dev. Cell* **12,** 467–474 (2007).
11. Rusan, N. M. & Peifer, M. A role for a novel centrosome cycle in asymmetric cell division. *J Cell Biol* **177,** 13–20 (2007).
12. Januschke, J. *et al.* Centrobin controls mother–daughter centriole asymmetry in Drosophila neuroblasts. *Nat. Cell Biol.* **15,** 241–248 (2013).
13. Ramdas Nair, A. *et al.* The Microcephaly-Associated Protein Wdr62/CG7337 Is Required to Maintain Centrosome Asymmetry in Drosophila Neuroblasts. *Cell Rep* **14,** 1100–1113 (2016).
14. Singh, P., Ramdas Nair, A. & Cabernard, C. The Centriolar Protein Bld10/Cep135 Is Required to Establish Centrosome Asymmetry in Drosophila Neuroblasts. *Curr. Biol.* **24,** 1548–1555 (2014).
15. Lerit, D. A. & Rusan, N. M. PLP inhibits the activity of interphase centrosomes to ensure their proper segregation in stem cells. *J Cell Biol* **202,** 1013–1022 (2013).
16. Lerit, D. A. *et al.* Interphase centrosome organization by the PLP-Cnn scaffold is required for centrosome function. *J. Cell Biol.* **210,** 79–97 (2015).
17. Nigg, E. A. & Stearns, T. The centrosome cycle: Centriole biogenesis, duplication and inherent asymmetries. *Nat. Cell Biol.* **13,** 1154–1160 (2011).
18. Fu, J., Hagan, I. M. & Glover, D. M. The Centrosome and Its Duplication Cycle. *Cold Spring Harb Perspect Biol* **7,** (2015).
19. Fu, J. *et al.* Conserved molecular interactions in centriole-to-centrosome conversion. *Nat. Cell Biol.* (2015). doi:10.1038/ncb3274
20. Novak, Z. A., Conduit, P. T., Wainman, A. & Raff, J. W. Asterless Licenses Daughter Centrioles to Duplicate for the First Time in Drosophila Embryos. *Current Biology* **24,** 1276–1282 (2014).
21. Buszczak, M. *et al.* The carnegie protein trap library: a versatile tool for Drosophila developmental studies. *Genetics* **175,** 1505–1531 (2007).
22. Nicholas, A. K. *et al.* WDR62 is associated with the spindle pole and is mutated in human microcephaly. *Nat Genet* **42,** 1010–1014 (2010).
23. Bacino, C. A., Arriola, L. A., Wiszniewska, J. & Bonnen, P. E. WDR62 missense mutation in a consanguineous family with primary microcephaly. *American journal of medical genetics. Part A* **158A,** 622–625 (2012).
24. Rupp, V., Rauf, S., Naveed, I., Windpassinger, C. & Mir, A. A novel single base pair duplication in WDR62 causes primary microcephaly. *BMC Med. Genet.* **15,** 107 (2014).

25. Gillingham, A. K. & Munro, S. The PACT domain, a conserved centrosomal targeting motif in the coiled-coil proteins AKAP450 and pericentrin. *EMBO Rep.* **1,** 524–529 (2000).
26. Saerens, D. *et al.* Identification of a Universal VHH Framework to Graft Non-canonical Antigen-binding Loops of Camel Single-domain Antibodies. *J. Mol. Biol.* **352,** 597–607 (2005).
27. Caussinus, E., Kanca, O. & Affolter, M. Fluorescent fusion protein knockout mediated by anti-GFP nanobody. *Nat Struct Mol Biol* **19,** 117–121 (2011).
28. Moutinho Santos, T., Sampaio, P., Amorim, I., Costa, M. & Sunkel, C. E. In vivo localisation of the mitotic POLO kinase shows a highly dynamic association with the mitotic apparatus during early embryogenesis in Drosophila. *Biology of the Cell* **91,** 585–596 (1999).
29. Albertson, R. & Doe, C. Q. Dlg, Scrib and Lgl regulate neuroblast cell size and mitotic spindle asymmetry. *Nat. Cell Biol.* **5,** 166–170 (2003).
30. Blachon, S. *et al.* A proximal centriole-like structure is present in Drosophila spermatids and can serve as a model to study centriole duplication. *Genetics* **182,** 133–144 (2009).
31. Stevens, N. R., Dobbelaere, J., Brunk, K., Franz, A. & Raff, J. W. Drosophila Ana2 is a conserved centriole duplication factor. *J. Cell Biol.* **188,** 313–323 (2010).
32. Megraw, T. L., Kilaru, S., Turner, F. R. & Kaufman, T. C. The centrosome is a dynamic structure that ejects PCM flares. *Journal of cell science* **115,** 4707–4718 (2002).
33. Blachon, S. *et al.* Drosophila asterless and vertebrate Cep152 Are orthologs essential for centriole duplication. *Genetics* **180,** 2081–2094 (2008).
34. Cabernard, C. *et al.* Apical/basal spindle orientation is required for neuroblast homeostasis and neuronal differentiation in Drosophila. *Dev. Cell* **17,** 134–141 (2009).
35. Gratz, S. J. *et al.* Genome engineering of Drosophila with the CRISPR RNA-guided Cas9 nuclease. *Genetics* **194,** 1029–1035 (2013).
36. Ren, X. *et al.* Enhanced Specificity and Efficiency of the CRISPR/Cas9 System with Optimized sgRNA Parameters in Drosophila. *Cell Rep* **9,** 1151–1162 (2014).

Acknowledgements:

We thank members of the Cabernard lab for helpful discussions. We are grateful to Jordan Raff, Nasser Rusan, Tomer Avidor-Reiss, Cayetano Gonzalez and Chris Doe for flies and antibodies. We would also like to thank the Imaging Core Facility (IMCF) at the Biozentrum for technical support and the Nigg lab for providing temporary lab space to E. G. This work was supported by the Swiss National Science Foundation (SNSF) and start-up funds from the University of Washington. E.G was supported with an EMBO long-term postdoctoral fellowship (ALTF 378-2015). Stocks obtained from the Bloomington Drosophila Stock Center (NIH P40OD018537) and the Vienna Drosophila Resource Center (VDRC) were used in this study.

Author contributions:

This study was conceived by A.R.N, P.S, and C.C.

E.G and A.R.N performed most of the experiments with help from P.S.

A. M generated the PACT::vhhGFP4 construct. T.P wrote custom-made Matlab codes and helped with data analysis. D.S.G generated the Plp CRISPR line and A.F helped with 3D-SIM imaging. E.G, A.R.N and C.C wrote the paper.

Competing financial interests: The authors declare no competing financial interests.

Materials & Correspondence. Material requests and other inquiries should be directed to ccabern@uw.edu.

348 **Figures**

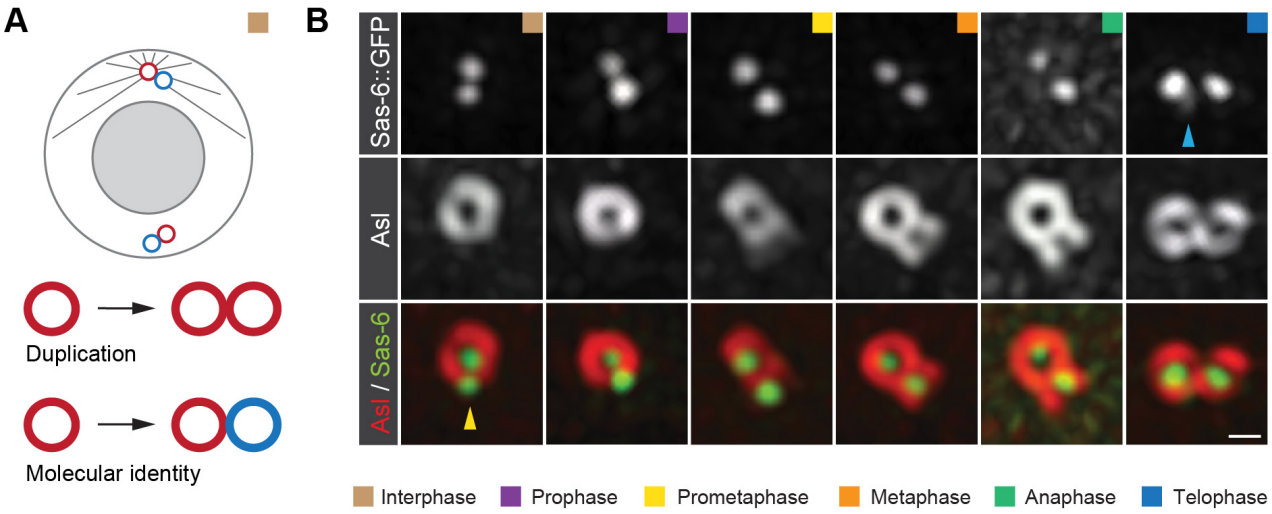

349

350

351 **Figure 1: Neuroblast centriole duplication completes in mitosis**

352 **(A)** Neuroblast centrosomes are inherently asymmetric in interphase but when neuroblast centrioles
353 duplicate and acquire a unique molecular identity (indicated by arrow and color switch) is unknown. **(B)**
354 Representative interpolated 3D-SIM images of third instar larval neuroblast centrosomes, expressing Sas-
355 6::GFP (top row; white. Green in merge) and stained for Asl (middle row; white. Merged channels; red).
356 The yellow arrowhead highlights the cartwheel of the forming centriole. Cartwheel duplication can be
357 observed at the telophase/interphase transition, concomitantly with centrosome separation (blue
358 arrowhead). Cell cycle stages are indicated with colored boxes. Scale bar is 0.3 μm.

359

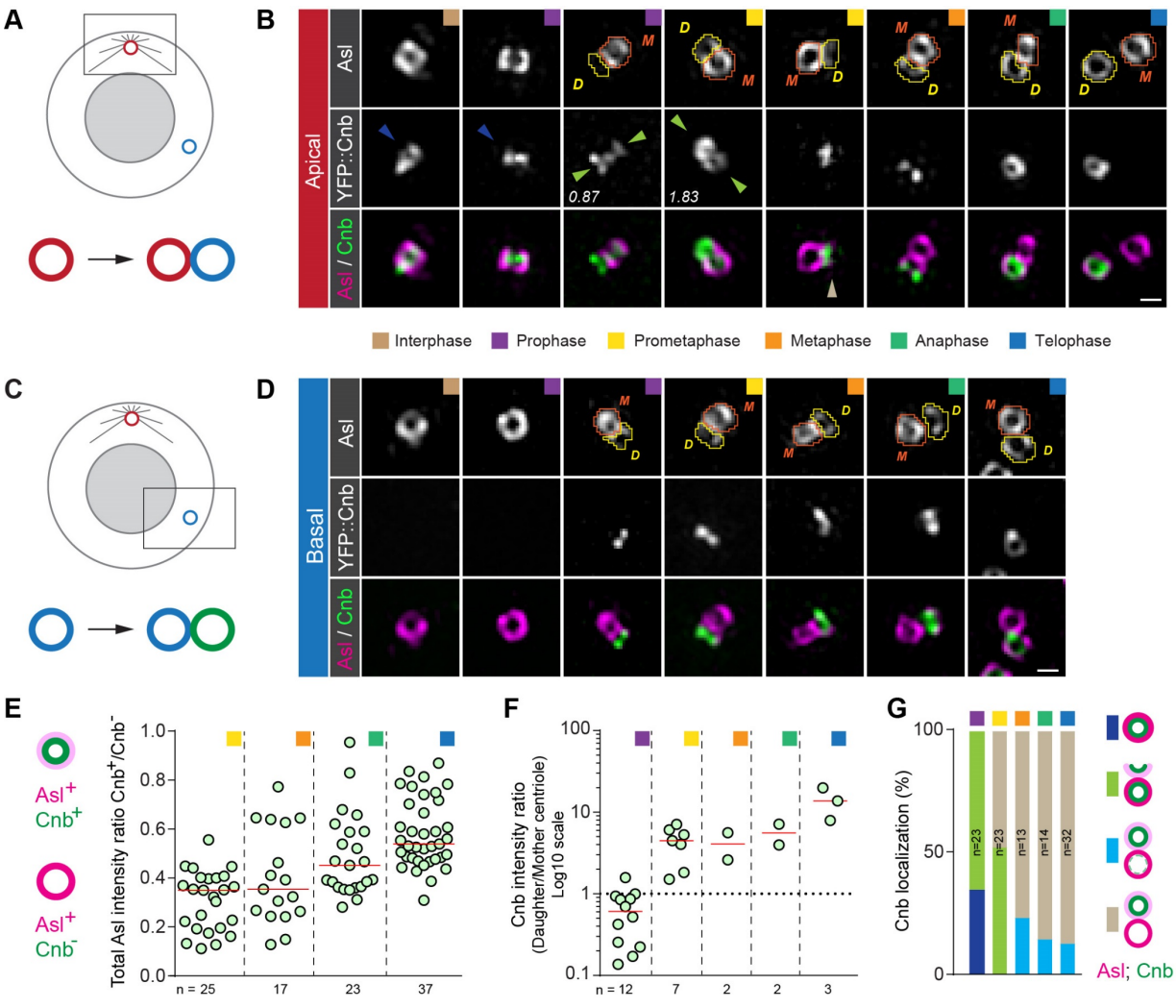

Figure 2: Cnb switches from the mother to the daughter centriole in early mitosis on the apical centrosome

How centriole duplication and molecular asymmetry are coupled is unclear for both the apical **(A)** and basal **(C)** centrosome. Representative 3D-SIM images of an apical **(A)** and basal **(D)** third instar neuroblast centrosome, expressing YFP::Cnb (middle row; white. Green in merge) and stained for Asl (Top row; white. Magenta in merge). Orange and yellow shapes highlight mother and daughter centrioles, respectively. The numbers indicate the total Cnb asymmetry ratios (Daughter/Mother centriole). Colored arrowheads highlight the different stages shown in (G; see also Figure S3B). **(E)** For prometaphase to telophase centrioles (apical and basal centrosomes combined), containing a single Cnb^{+} centriole, total Asl

intensity of the Cnb^{+} (presumably the daughter) centriole was divided by the total Asl intensity of the Cnb^{-} (presumably the mother) centriole. Medians are shown with a red horizontal line. **(F)** Scatter plot showing total Cnb intensity of the daughter centriole (less Asl), divided by total Cnb intensity on the mother centriole (more Asl). Only apical centrioles containing Cnb on both centrioles were measured. **(G)** Graph showing the timeline of Cnb's relocalization to the apical centrosome: the bars show the percentage of neuroblasts containing a single Cnb^{+} centriole (dark blue), Cnb on both centrioles (transition stage; light green), predominant Cnb localization on the daughter centriole (strong asymmetry; light blue) or in which Cnb is completely shifted to the daughter centriole (brown) at defined mitotic stages. For this and all subsequent cartoons: closed and open circles represent completed and incompleted centriole duplications, respectively. Cell cycle stages are indicated with colored boxes. Scale bar is 0.3 μm. The data presented here were obtained from five independent experiments.

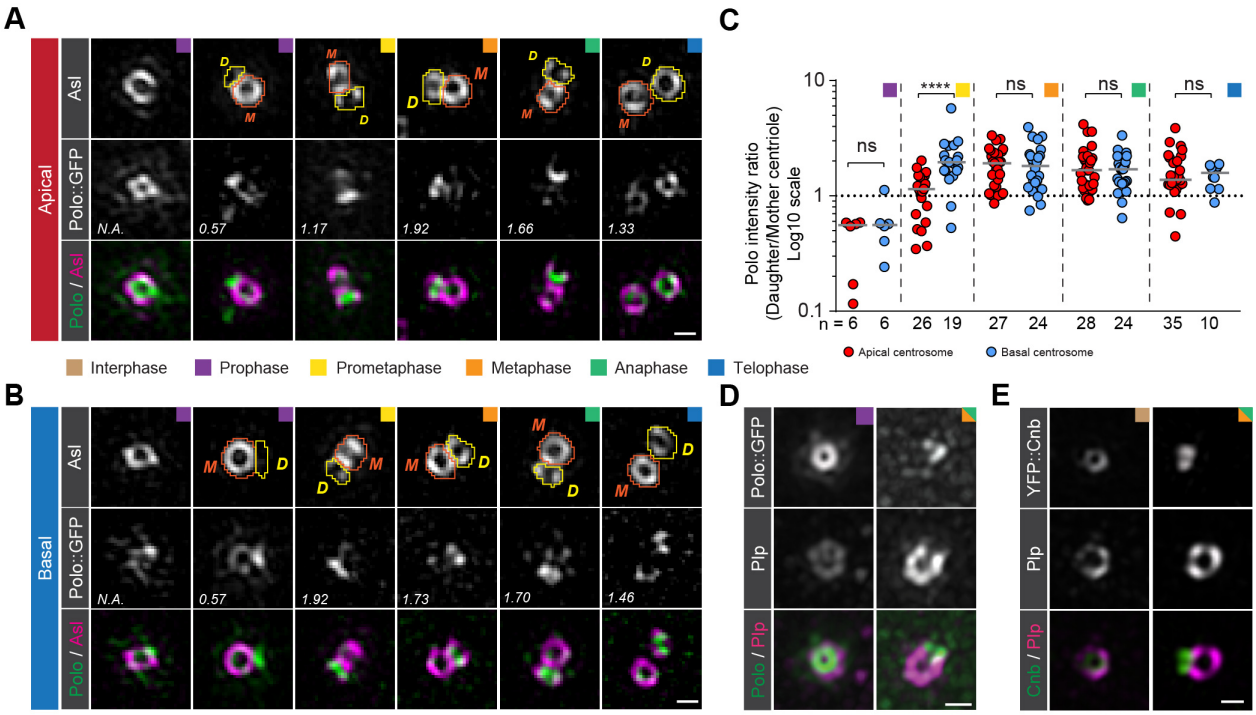

Figure 3: Polo and Cnb separate from Plp in mitosis

Representative 3D-SIM images of **(A)** apical or **(B)** basal third instar larval neuroblast centrioles, expressing Polo::GFP (middle row; green in merge). Centriole contours were drawn based on Asl signal (orange and yellow lines for mother and daughter centriole respectively) and used to measure Polo (and Asl; not shown) intensities. The numbers represent total Polo intensity ratios (Daughter/Mother centriole) in the shown image. Polo asymmetry ratios for the apical (red dots) and the basal (blue dots) centrosome are plotted in **(C)** from three independent experiments. Medians are shown with a grey horizontal line. Prophase: apical versus basal; p=0.6991. Prometaphase: apical versus basal; $p=5.688x10^{-6}$. Metaphase: apical versus basal; p=0.9329. Anaphase: apical versus basal; p=0.8628. Telophase: apical versus basal: p=0.8614. Representative interpolated images of apical interphase/early prophase and late metaphase/early anaphase centrosomes, expressing **(D)** Polo::GFP (green in merge) or **(E)** YFP::Cnb (green in merge) and stained for Plp (magenta in merge). These experiments were performed three times independently for Polo::GFP and once for YFP::Cnb. Cell cycle stages are indicated with colored boxes. Scale bar is 0.3 µm.

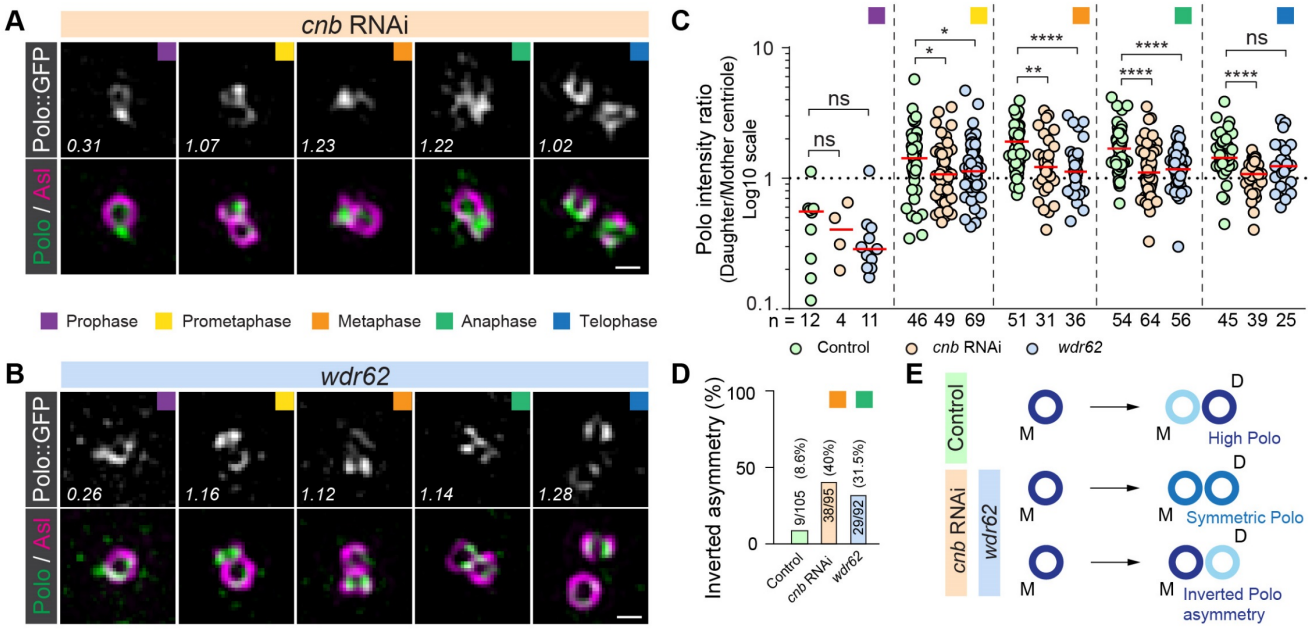

Figure 4: Cnb and Wdr62 are required to establish centrosome asymmetry in mitosis.

Representative 3D-SIM images of third instar larval neuroblast centrosomes, expressing **(A)** RNAi against Cnb (*cnb* RNAi) or **(B)** mutant for *wdr62*. In both conditions, Polo::GFP (green in merge) expressing neuroblasts were stained for Asl (magenta in merge). Polo intensity ratios (Daughter/Mother centriole) are shown in the representative images and plotted in **(C)** for control (wild type background; green dots), *cnb* RNAi (beige dots) and *wdr62* mutants (blue dots). Since apical and basal centrosomes could not be distinguished in *cnb* RNAi and *wdr62* mutants, measurements from these conditions were compared to the pooled (apical and basal) control Polo measurements (replotted from Figure 3C). These experiments were performed three times independently for wild type control and *cnb* RNAi, and six times for *wdr62*. Prophase: wild type control versus *cnb* RNAi; p=0.6835. wild type control versus *wdr62*; p=0.1179. Prometaphase: wild type control versus *cnb* RNAi; p=0.0318. wild type control versus *wdr62*; p=0.0439. Metaphase: wild type control versus *cnb* RNAi; p=0.0040; wild type control versus *wdr62*; $p=8.496\times10^{-5}$. Anaphase: wild type control versus *cnb* RNAi; $p=4.19\times10^{-6}$. wild type control versus *wdr62*; $p=1.79\times10^{-6}$. Telophase: wild type control versus *cnb* RNAi; $p=1.17\times10^{-6}$. wild type control versus *wdr62*; p=0.0524. The percentage of metaphase and anaphase centrosomes with inverted Polo asymmetry are plotted in **(D)**.

413 **(E)** Summary of phenotypes; in neuroblasts lacking Cnb or Wdr62, Polo often fails to transfer from the
414 mother (M) to the daughter (D) centriole, resulting in symmetric or inverted asymmetric Polo localization.
415 Cell cycle stages are indicated with colored boxes. Scale bar is 0.3 μm.
416

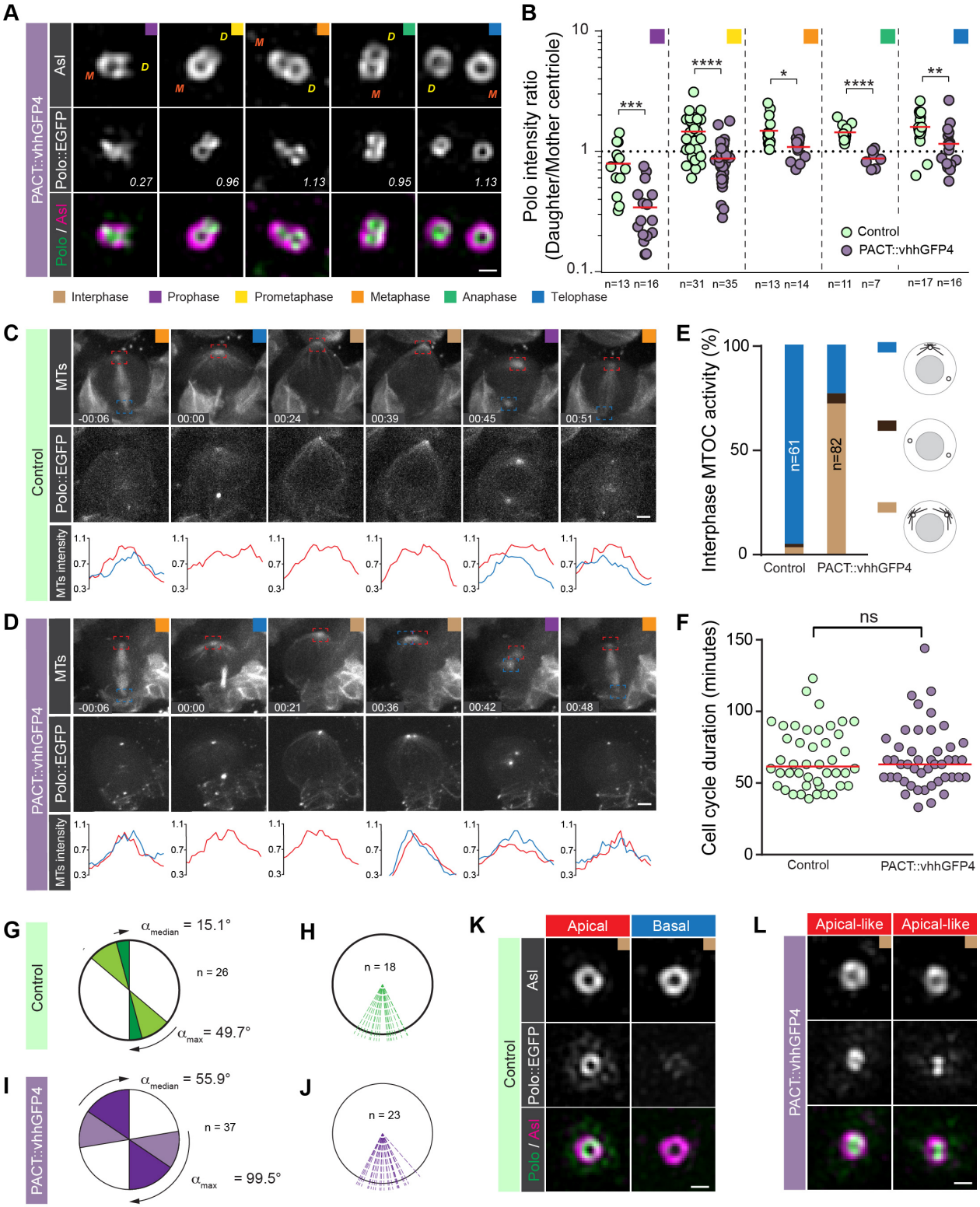

Figure 5: The centrosome asymmetry switch is required for biased interphase MTOC activity and centrosome positioning.

(A) Representative 3D-SIM images of third instar larval neuroblast centrosomes, expressing Polo::EGFP (generated by CRISPR/Cas9) and the nanobody construct PACT::vhhGFP4. Polo::EGFP (green in the merge) expressing neuroblasts were stained for Asl (magenta in the merge). Polo intensity ratios (Daughter/Mother centriole) are plotted in **(B)** for Control (green dots) and PACT::vhhGFP4 (purple dots). These experiments were performed 2 times independently in parallel for both genotypes. Prophase: Control versus PACT::vhhGFP4; $p=3.11x10^{-4}$. Prometaphase: Control versus PACT::vhhGFP4; $p=3.49x10^{-6}$. Metaphase: Control versus PACT::vhhGFP4; p=0.0222. Anaphase: Control versus PACT::vhhGFP4; $p=6.28x10^{-5}$. Telophase: Control versus PACT::vhhGFP4; p=0.0077. **(C)** Representative live cell imaging time series of a dividing control (Polo::EGFP, worGal4, UAS-mCherry::Jupiter expressing wild type flies) and PACT::vhhGFP4 (together with worGal4, UAS-mCherry::Jupiter) **(D)** neuroblast. The microtubule marker (MTs, first row) and Polo::EGFP (second row) are shown for two consecutive mitoses. Microtubule intensity of the apical (red line and square) and basal (blue line and square) MTOC are plotted below. "00:00" corresponds to the telophase of the first division. **(E)**. Bar graph showing the quantification of the MTOC phenotype. Cell cycle length is shown in **(F)**. The cell cycle length in PACT::vhhGFP4 (purple dots) is not significantly different from the control (green dots); p=9727. **(G)** and **(I)** represent the spindle rotation between NEBD and anaphase. Medians are displayed in dark colors (green; control. Purple; vhhGFP4 expressing neuroblasts) and the maximum rotation in light colors. Division orientation between consecutive mitoses shown for control **(H)** and PACT::vhhGFP4 **(J)**. **(K)** and **(L)** are representative 3D-SIM images of interphase centrosomes for control and PACT::vhhGFP4 expressing neuroblasts, respectively. The trapping of Polo::EGFP with PACT::vhhGFP4 induces two identical apical-like centrosomes with a strong centriolar and PCM signal. The data presented for the live imaging here were obtained from five independent experiments. Cell cycle stages are indicated with colored boxes.

Yellow "D" and orange "M" refer to Daughter and Mother centrioles based on Asl intensity. Timestamps are shown in hh:mm and scale bar is 0.3µm (A, K, L) and 3 µm (C,D), respectively.

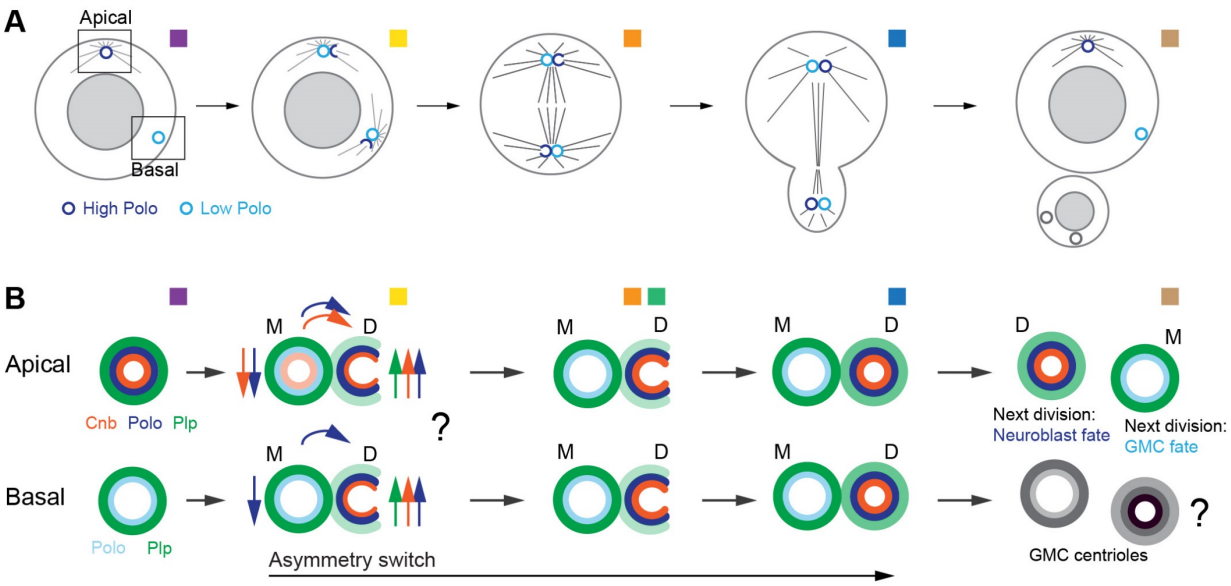

Figure 6: Model

(A) The centrosome asymmetry switch – here shown for Polo (dark and light blue, respectively) – occurs during mitosis, coupled to centriolar wall completion. Polo is relocalizing from the existing mother to the newly formed daughter centriole on both the apical and basal centrosome. This asymmetry switch causes the Polo-rich centriole to maintain MTOC activity, retaining it in the self-renewed neuroblast. Details for the apical and basal centrosome are shown in **(B)**. Cnb (orange) and Polo (blue) relocalize from the mother to the forming daughter centriole from prophase onwards. The basal centrosome only switches Polo but directly upregulates Cnb on the daughter centriole; protein upregulation (vertical arrows) could act in parallel to direct protein transfer (curved arrows). Plp remains on the mother, potentially increasing in intensity and appearing on the daughter centriole in prometaphase. The centrosome asymmetry switch is mostly completed by anaphase. The centriole containing less Plp, gained Cnb and Polo and is destined to be inherited by the self-renewed neuroblast in the next division, whereas the centriole containing higher Plp and lower Polo levels is destined to be inherited by the GMC. The fate of the basal centrioles and subsequent marker distribution is unknown (represented by grey circles).

Materials and Methods

Fly strains and genetics:

The following mutant alleles and transgenes were used: CnbRNAi (VDRC, 28651GD), *wdr62*$^{\Delta 3\text{-}9}$ allele [13], *Df(2L)Exel8005* (a deficiency removing the entire *wdr62* locus and adjacent genes; Bloomington Drosophila Stock Center), *worniu-Gal4* [29], *pUbq-DSas-6::GFP* [30], *pUbq-GFP::Ana-2* [31], Cnn::GFP [32], *Polo::GFP*^{CC01326} (protein trap line [21]), *GFP::Polo* (genomic rescue construct using Polo's endogenous enhancer) [28], *Polo::EGFP* (generated by CRISPR; this work), *pUbq-Asl::GFP* and *pUbq-Ana-1::GFP* [33], *Plp::EGFP* (this work), *pUbq-YFP::Cnb* [6], *Bld10::GFP* [33], *nos-Cas9/Cyo* (Bloomington Drosophila Stock Center), *y*^{1} *w*^{67c23} *P{y[+mDint2]=Crey}1b; D/TM3, Sb*^{1} (Bloomington Drosophila Stock Center), worGal4, UAS-mCherry::Jupiter [34].

Generation of transgenes using CRISPR/Cas9:

Plp::EGFP was generated with CRISPR/Cas9 technology. Two target-specific sequences with high efficiency were chosen using the CRISPR Optimal Target Finder (http://tools.flycrispr.molbio.wisc.edu/targetFinder/), and the DRSC CRISPR finder and Efficiency Predictor (http://www.flyrnai.org/crispr/), (http://www.flyrnai.org/evaluateCrispr/) web tools. Sense and antisense primers (first target site: CTTCGAACTAGCGTCCACAAGGTC and AAACGACCTTGTGGACGCTAGTTC; second target site: AAACGACCTTGTGGACGCTAGTTC and AAACGACCTTGTGGACGCTAGTTC) were cloned into pU6-BbsI-ChiRNA [35] between BbsI sites. To generate the replacement donor template, 1kb homology arms flanking the target sequences and two "repair sequences" (to reintroduce the sequence flanking the STOP codon, in between the target sequences) were cloned into pHD-EGFP-DsRed. This vector was generated by inserting EGFP sequence flanked by attP sites and fused to a LoxP site, between NdeI and BsiWI sites in pHD-DsRed-attP vector (gift from Melissa Harrison & Kate O'Connor-Giles & Jill Wildonger (Addgene plasmid # 51019)).

Polo::EGFP was generated with a similar strategy. The following sense and antisense primers were used: first target site CTTCGTCAGTCACCTCGGTGAATAT and AAACATATTCACCGAGGTGACTGAC. Second target site CTTCGAGACTGTAGGTGACGCATTC and AAACGAATGCGTCACCTACAGTCTC. Embryos expressing *nos-Cas9* [36] were injected with two pU6-ChiRNA vectors and the pHD-EGFP-DsRed and successful events were detected by screening for DsRed-positive eyes in F1 generation. Constitutively active Cre (Bloomington Drosophila Stock Center) was crossed in to remove the DsRed marker. Positive events were genotyped and sequenced.

Generation of PACT::HA::vhhGFP4

The coding sequence of PACT [25] and vhhGFP4 [26] were PCR amplified and cloned into a pUAST-attB vector using In-Fusion technology (Takara, Clontech). HA was added by using primers containing the HA sequence. The resulting construct was injected into attP (VK00027 and VK00037; Bestgene).

Immunohistochemistry:

The following antibodies were used for this study: rat anti-α-Tub (Serotec; 1:1000), mouse anti-α-Tub (DM1A, Sigma; 1:2500), rabbit anti-Asl (1:500), rabbit anti-Plp (1:1000) (gifts from J. Raff). Secondary antibodies were from Molecular Probes and the Jackson Immuno laboratory.

Antibody staining:

96-120h (AEL; after egg laying) larval brains were dissected in Schneider's medium (Sigma) and fixed for 20 min in 4% paraformaldehyde in PEM (100mM PIPES pH 6.9, 1mM EGTA and 1mM MgSO4). After fixing, the brains were washed with PBSBT (1X PBS, 0.1% Triton-X- 100 and 1% BSA) and then blocked with 1X PBSBT for 1h. Primary antibody dilution was prepared in 1X PBSBT and brains were incubated for up to 2 days at 4 °C. Brains were washed with 1X PBSBT four times for 20 minutes each and then

incubated with secondary antibodies diluted in 1X PBSBT at 4 °C, overnight. The next day, brains were washed with 1X PBST (1x PBS, 0.1% Triton-X- 100) four times for 20 minutes each and kept in Vectashield H-1000 (Vector laboratories) mounting media at 4 °C.

Super–Resolution 3D Structured Illumination Microscopy (3D-SIM):

3D-SIM was performed on fixed brain samples using a DeltaVision OMX-Blaze system (version 4; GE Healthcare), equipped with 405, 445, 488, 514, 568 and 642 nm solid-state lasers. Images were acquired using a Plan Apo N 60x, 1.42 NA oil immersion objective lens (Olympus) and 4 liquid-cooled sCMOs cameras (pco Edge, full frame 2560 x 2160; Photometrics). Exciting light was directed through a movable optical grating to generate a fine-striped interference pattern on the sample plane. The pattern was shifted laterally through five phases and three angular rotations of 60° for each z section. Optical z-sections were separated by 0.125 µm. The laser lines 405, 488, 568 and 642 nm were used for 3D-SIM acquisition. Exposure times were typically between 3 and 100 ms, and the power of each laser was adjusted to achieve optimal intensities of between 5,000 and 8,000 counts in a raw image of 15-bit dynamic range at the lowest laser power possible to minimize photobleaching. Multichannel imaging was achieved through sequential acquisition of wavelengths by separate cameras.

3D-SIM Image Reconstruction:

Raw 3D-SIM images were processed and reconstructed using the DeltaVision OMX SoftWoRx software package (GE Healthcare; Gustafsson, M. G. L. 2000). The resulting size of the reconstructed images was of 512 x 512 pixels from an initial set of 256 x 256 raw images. The channels were aligned in the image plane and around the optical axis using predetermined shifts as measured using a target lens and the SoftWoRx alignment tool. The channels were then carefully aligned using alignment parameter from control measurements with 0.5 µm diameter multi-spectral fluorescent beads (Invitrogen, Thermo Fisher Scientific).

Diameter measurements method:

Maximum projection of centrioles were aligned in *x,y* and segmented using a custom-made MatLab code. Centroids for both inner and outer centriole rings were determined and the mean inner and outer radii were calculated by averaging the distance from the centroid to all the edge pixels, respectively. Dot like-structures were measured with a similar method. If dots appeared fused, the centroid for each dot was first determined by removing the overlapping region using a high threshold value. A lower background threshold value was used to distinguish the centriole's outer boundary from surrounding background. The radial distance from each centroid to all the edge pixels of the centriole's outer boundary was then calculated. To accurately measure the mean radius of a centriole that has an overlapping region with another centriole, only the radial distance, revolving around the hemisphere of the selected centriole, was used for the calculation. The areas were measured using only pixels with an intensity value above the chosen background threshold.

Centriole age measurement method:

To determine centriolar age, Asl intensity was used as a reference. The contours of non-overlapping centrioles were drawn in ImageJ based on Asl signal and saved as XY coordinates. Using a custom-made MatLab code, the total intensities above the background threshold values (determined by the experimenter) for Asl were calculated in the drawn centriolar areas. Total Asl intensity was then used to determine centriolar age: daughter centrioles have lower intensity than mother centrioles. The same XY coordinates were used to measure total pixel intensity for markers of interest (e.g Polo::GFP, Plp::EGFP). Asymmetry ratios for markers of interest were then determined by dividing the total daughter centriole pixel intensity with total pixel intensity from the mother centriole, respectively.

Live cell imaging

96-120h (AEL; after egg laying) larval brains were dissected in Schneider's medium (Sigma-Aldrich, S0146) supplemented with 10% BGS (HyClone) and transferred to 50 µL wells (Ibidi, µ-Slide

564 Angiogenesis) for live cell imaging. Live samples were imaged on a Perkin Elmer spinning disk confocal
565 system "Ultra View VoX" with a Yokogawa spinning disk unit and two Hamamatsu C9100-50 frame
566 transfer EMCCD cameras. A 63x / 1.40 oil immersion objective mounted on a Leica DMI 6000B was used.
567 Brains form a given genotype and the corresponding control were imaged under temperature control (25°C)
568 in parallel. The time resolution was 3 minutes.
569
570 **Angle measurements**
571 Imaris' "Spot" tool was used to collect x, y and z coordinates of apical and basal centrosomes before NEBD
572 and at anaphase. These coordinates were used to calculate spindle rotation between NEBD and anaphase
573 onset and changes in division axis between successive anaphases.
574
575 **Statistical analysis:**
576 Statistical analyses were performed on Prism (GraphPad software). Statistical significance was assessed
577 with a two-sided non-parametric Mann-Whitney test to compare ranks between two samples with variable
578 variances and non-Gaussian distributions. P values < 0.05 were considered significant;
579 *; $p < 0.05$ **; $p < 0.01$; ***; $p < 0.001$; ****; $p < 0.0001$.
580
581 **Computer codes:**
582 Custom made Matlab codes used for data analysis are available upon request.
583
584 **Data availability:**
585 The authors declare that the data supporting the findings of this study are available within the paper and its
586 supplementary information files.
587

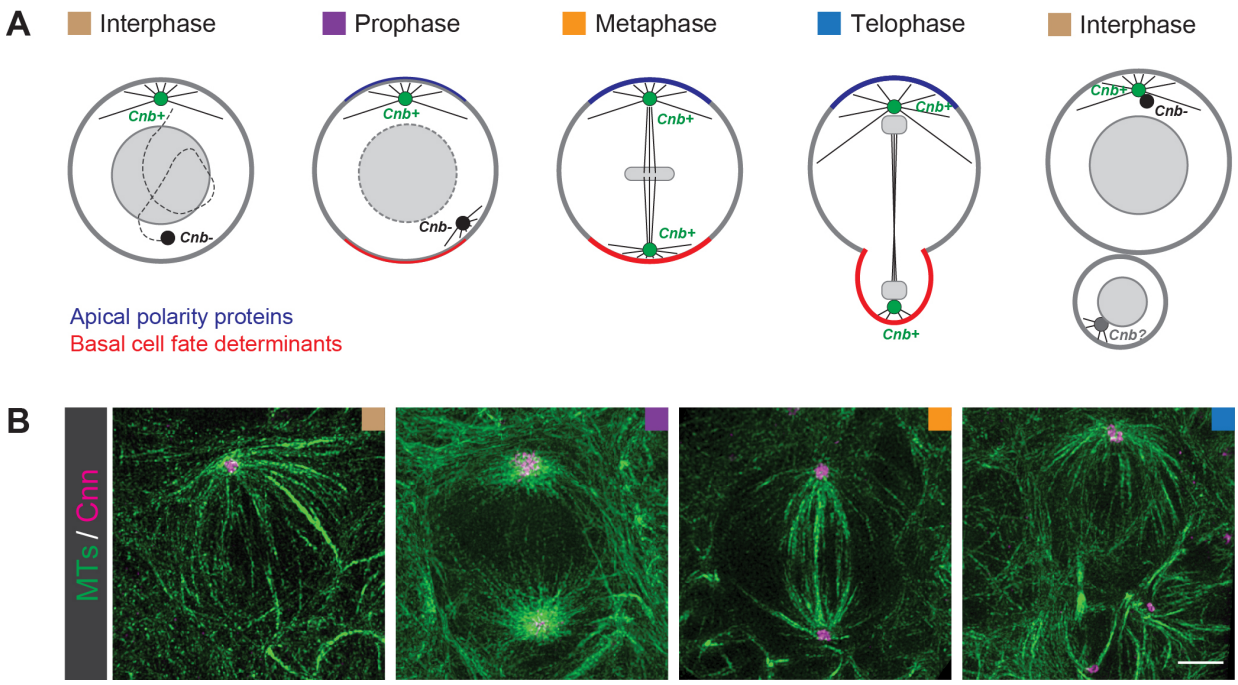

Figure S1: Neuroblast centrosomes are intrinsically asymmetric

(A) Current model of centrosome asymmetry in neuroblast. The Cnb^{+} apical daughter centrosome is active throughout interphase and constantly nucleates a robust microtubule array, maintaining its position at the apical neuroblast cortex (blue crescent). The Cnb^{-} basal mother centrosome is inactive during interphase, diffusing through the cytoplasm until it regains MTOC activity in prophase. At this point, the Cnb^{-} centrosome reached the basal side of the neuroblast and starts to reaccumulate Cnb during mitosis. The daughter centrosome is retained by the neuroblast and the mother centrosome is inherited by the differentiating GMC. Asymmetric centrosomes split in early interphase. **(B)** Representative 3D-SIM images of neuroblasts expressing the pericentriolar maker Cnn::GFP stained for α-Tubulin, labelling microtubules (MTs; green). The morphology of the microtubule array and cell shape were used to define neuroblast cell cycle stages. Scale bar is 3 μm. Colored boxes indicate cell cycle stages.

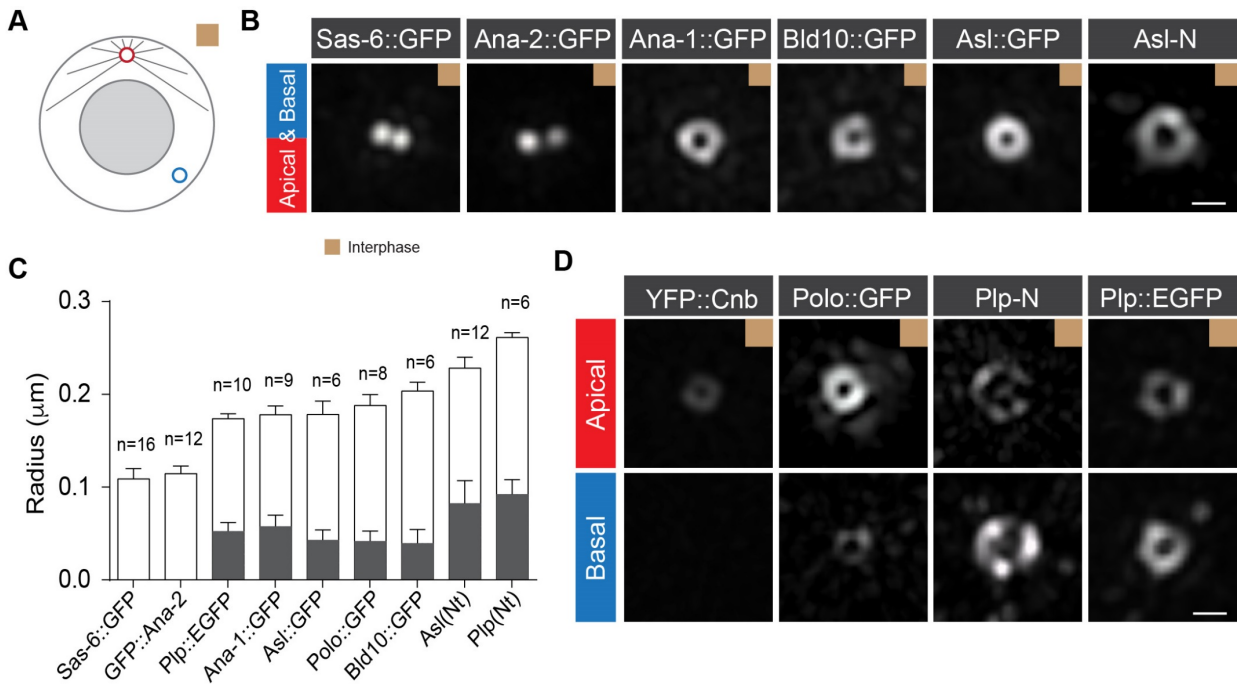

Figure S2: Centriolar proteins define centriole morphology and asymmetry

(A) Localization of centriolar markers was determined on apical (red circle) and basal (blue circle) centrosomes. **(B)** Representative, interpolated 3D-SIM images of interphase neuroblasts, expressing GFP-tagged centriolar markers or stained for Asl (recognizing Asl's N-terminus). **(C)** Radii measurements of centrosomal proteins. Outer (white) and inner (gray) radii are shown for proteins forming a ring-like structure. **(D)** Apical (red circle in (A)) and basal (blue circle in (A)) centrosomes, expressing or stained for centriolar markers, displaying asymmetric localization in interphase. Interpolated images are shown. Scale bar is 0.3 μm. Data was extracted from one to four independent experiments.

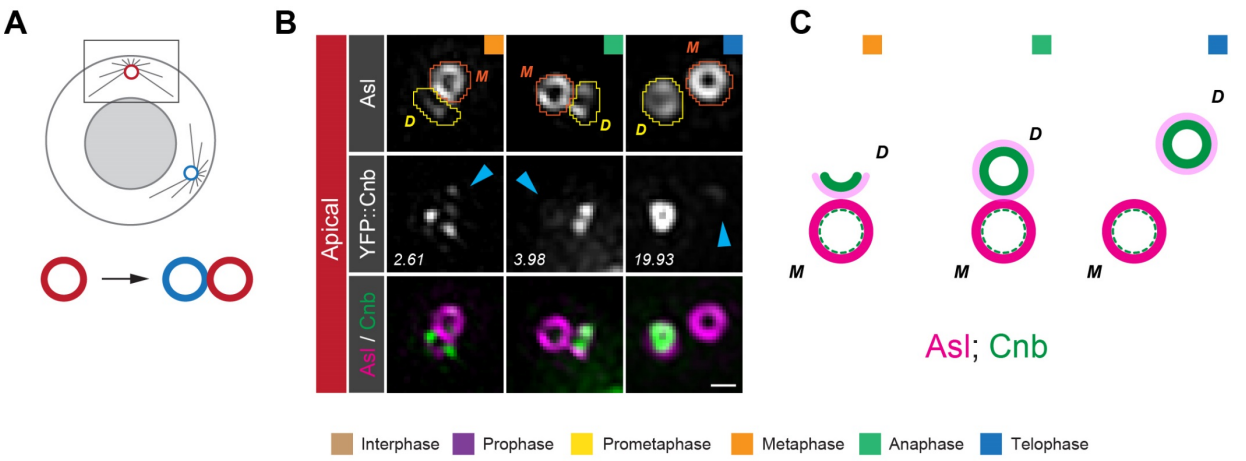

615

616

617 **Figure S3: Cnb switches from the mother to the daughter centriole in early mitosis**

618 **(A)** Cnb localization was analyzed on apical centrosomes (red circle). **(B)** In a few metaphase to telophase

619 neuroblasts, weak Cnb was also detectable on the mother centriole (light blue arrowheads). This class of

620 centrosomes is represented with the light blue bar in Figure 2G. **(C)** Cartoon, summarizing the findings

621 shown in (B). Scale bar is 0.3 µm. Colored boxes indicate cell cycle stages.

622

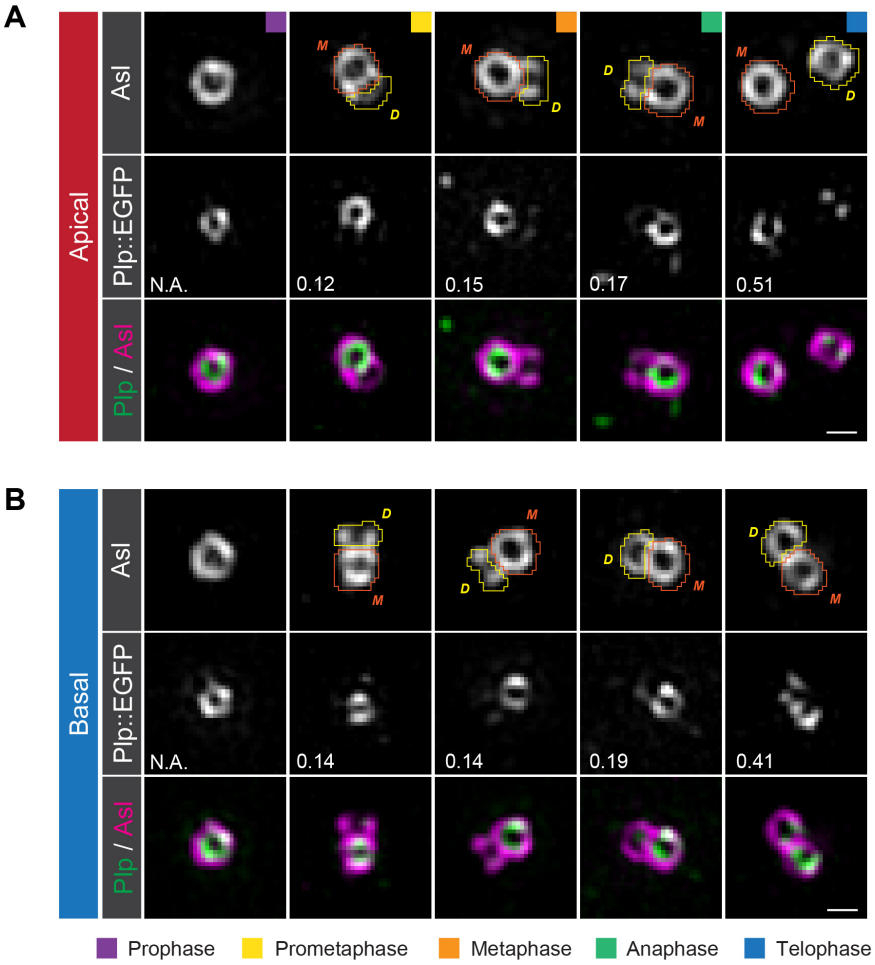

626 **Figure S4: Plp does not transfer but remains localized on the mother centriole**

627 Representative 3D-SIM images of **(A)** apical and **(B)** basal third instar larval neuroblast centrosomes,
628 expressing Plp::EGFP (middle row; green in merge), co-stained with Asl (white on top, magenta in merge).
629 The number represents total Plp intensity ratios (Daughter/Mother centriole) in the shown image. Plp
630 asymmetry ratios for the apical (red dots) and the basal (blue dots) centrosome are plotted in **(C)** from three
631 independent experiments. Medians are shown in dark grey. Prometaphase: apical versus basal; p=0.3856.
632 Metaphase: apical versus basal; p=0.2234. Anaphase: apical versus basal; p=0.3583. Telophase: apical
633 versus basal; p=0.1844. Plp does not switch its localization but remains localized on the mother centriole
634 on both centrosomes. Scale bar is 0.3 μm Colored boxes indicate cell cycle stages.
635

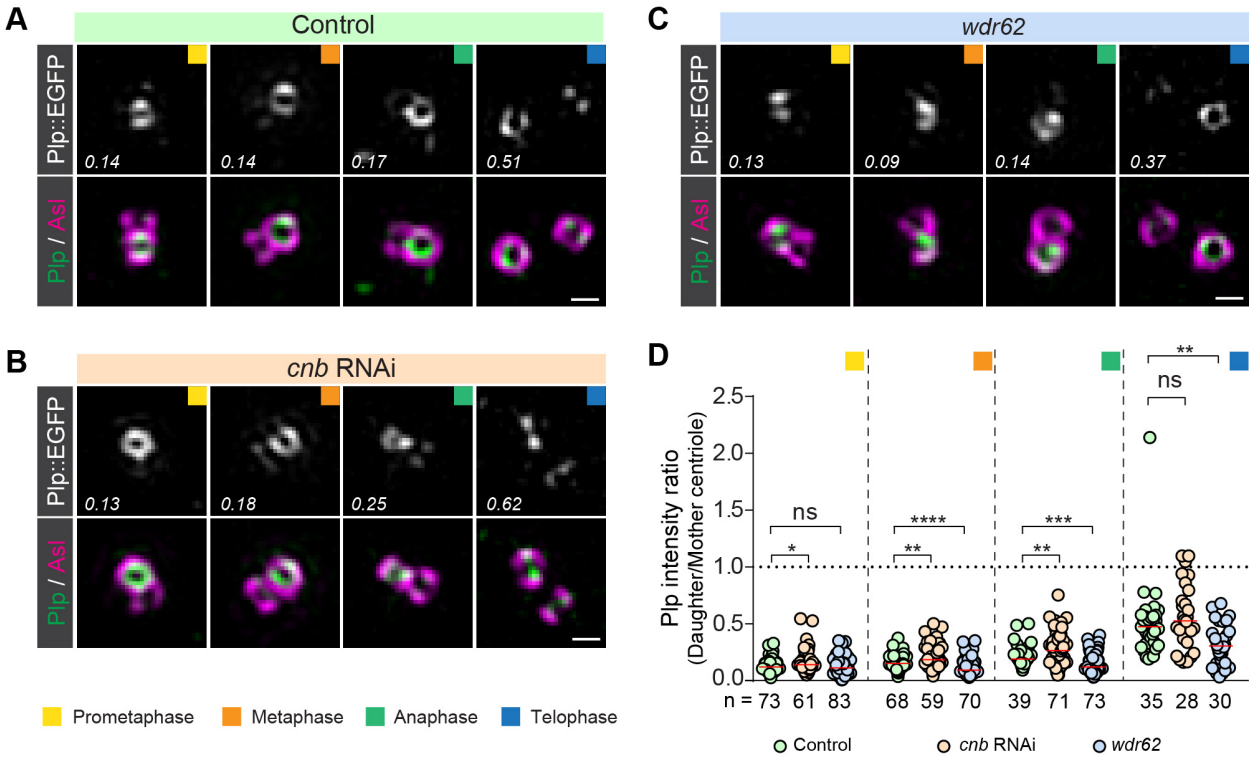

Figure S5: Cnb and Wdr62 are partially required to maintain and transfer Plp on the mother centriole

Representative 3D-SIM images of **(A)** wild type control, **(B)** *cnb* RNAi expressing or **(C)** *wdr62* mutant neuroblasts centrosomes, expressing endogenously tagged Plp (Plp::EGFP; green in the merge) stained for Asl (magenta in the merge). The number represents total Plp intensity ratios (Daughter/Mother centriole) in the shown image. Plp ratios (Daughter/Mother centriole) were plotted in **(D)**. Since apical and basal centrosomes could not be distinguished in *cnb* RNAi and *wdr62* mutants, measurements from these conditions were compared to the pooled (apical and basal) control Plp measurements (replotted from Figure S4C). Prometaphase: control versus *cnb* RNAi; p=0.0159. control versus *wdr62*; p=0.1175. Metaphase: control versus *cnb* RNAi; p=0.0025. control versus *wdr62*; $p=8.95x10^{-7}$. Anaphase: control versus *cnb* RNAi; p=0.0057. control versus *wdr62*; $p=1.61x10^{-4}$. Telophase: control versus *cnb* RNAi; p=0.2736. control versus *wdr62*; p=0.0019. Medians are shown in red. *cnb* RNAi mitotic centrosomes showed a weak but significant increase of their Plp intensity ratios from prometaphase until anaphase while *wdr62* mutant mitotic centrosomes displayed weak but significant decrease of their Plp ratio from metaphase onwards.

651 Scale bar is 0.3 μm. Colored boxes indicate cell cycle stages. These experiments were performed three

652 times independently for each genotype.

653
654

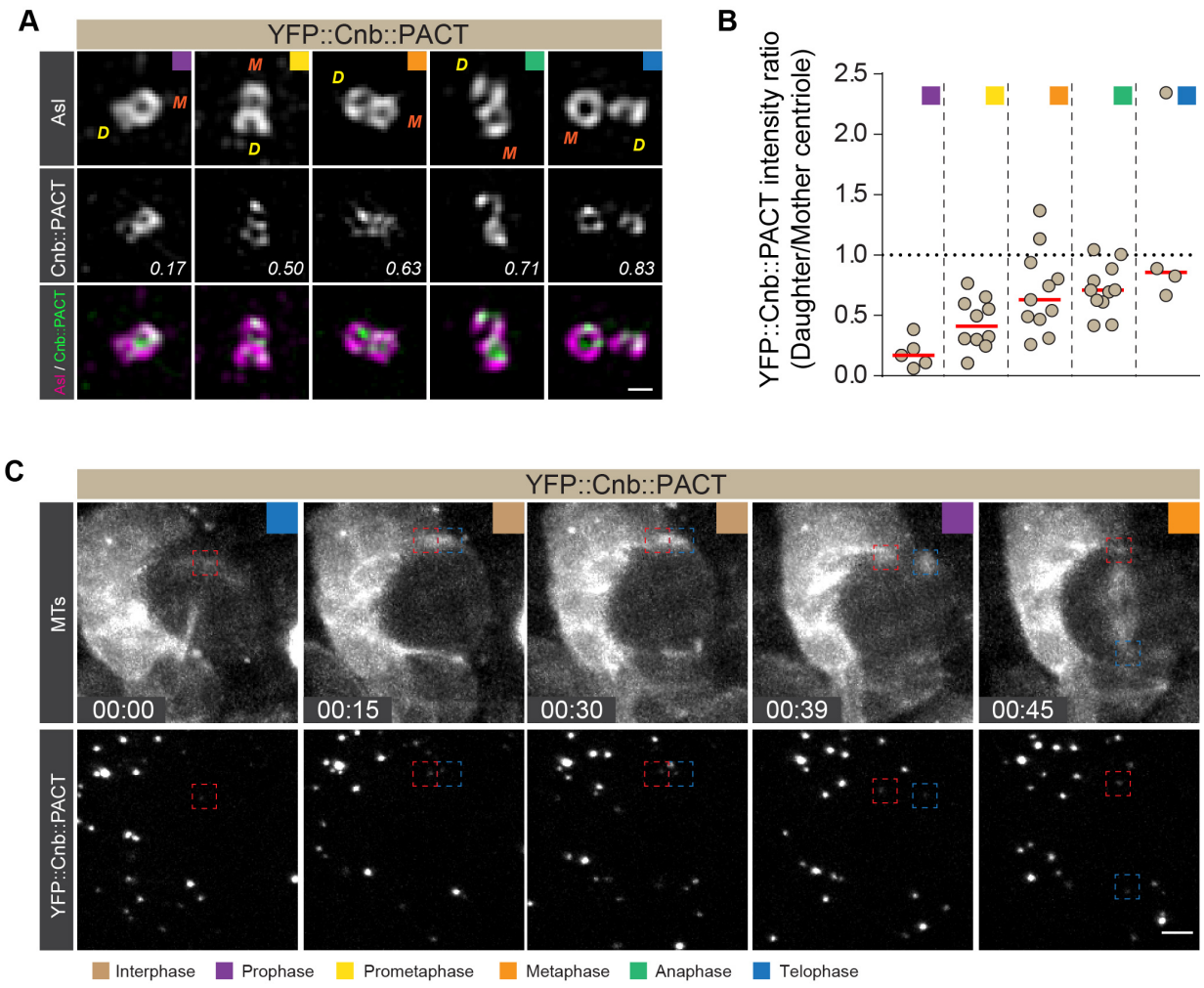

Figure S6: The ectopic localization of Cnb to both centrioles impairs Cnb to switch completely from the mother to the daughter centriole, affecting interphase MTOC activity

(A) Representative 3D-SIM images of third instar larval neuroblast centrosomes, expressing YFP::Cnb::PACT (white in the second row, green in the merge) and stained for Asl (white in the first row, magenta in the merge). The number represents total YFP::Cnb::PACT intensity ratios (Daughter/Mother centriole) in the shown image. YFP::Cnb::PACT Polo intensity ratios (Daughter/Mother centriole) from two experiments are plotted in **(B)**. **(C)** Representative live cell imaging series from a neuroblast, recorded in the intact brain, expressing the microtubule marker mCherry::Jupiter (MTs, first row) and YFP::Cnb::PACT (second row). Red and blue squares represent apical and basal centrosome respectively.

666 "00:00" corresponds to the telophase of the first division. Cell cycle stages are indicated with colored boxes.
667 Yellow "D" and orange "M" refer to Daughter and Mother centrioles based on Asl intensity. Timestamps
668 are shown in hh:mm and scale bar is 0.3μm (A) and 3 μm (C), respectively.
669

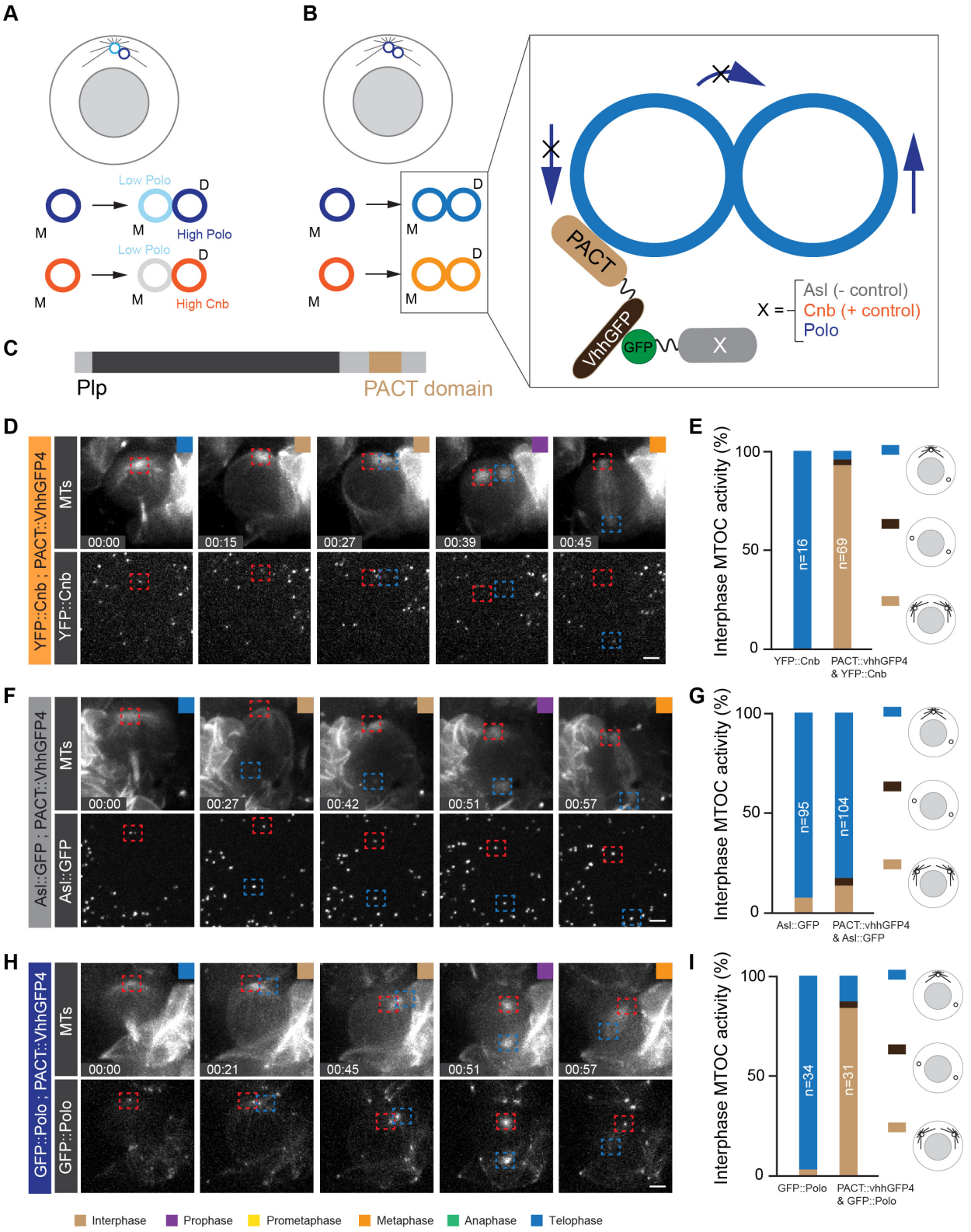

672 **Figure S7: Perturbing centriolar asymmetry by expressing the GFP-trapping nanobody to the**
673 **mother centriole**

674 **(A**) To test the function of the centrosome asymmetry switch, the relocalization of Polo and Cnb needs to
675 be perturbed. **(B)** Nanobody technology was used to prevent the centrosome asymmetry switch for selected
676 proteins of interest. The vhhGFP4 nanobody specifically traps GFP or YFP tagged proteins. By tethering
677 the nanobody preferentially to the mother centriole - using Plp's PACT domain **(C)**, we can perturb the
678 relocalization of GFP or YFP tagged centrosomal proteins. Crossed-out arrows illustrate a lack of centriolar
679 protein (shown for Polo; blue) relocalization. Representative live cell image series from intact brains for
680 neuroblasts expressing the microtubule marker mCherry::Jupiter (first row), together with **(D)** YFP::Cnb
681 and PACT::vhhGFP4, **(F)** Asl::GFP and PACT::vhhGFP4 or **(H)** GFP::Polo transgene (genomic rescue
682 construct; see methods) and PACT::vhhGFP4. MTOC quantifications are shown for YFP::Cnb **(E),**
683 Asl::GFP **(G)** and GFP::Polo **(I)**. "00:00" corresponds to telophase of the previous division. Cell cycle
684 stages are indicated with colored boxes. The data presented here were obtained from two, four and three
685 independent experiments for YFP::Cnb, Asl::GFP and GFP::Polo respectively. Timestamps are hh:mm and
686 scale bar is 3μm.

687

688 **Movie legends**

689

690 **Movie 1: Wild type control movie**

691 Wild type control larval neuroblast expressing the centriolar marker YFP::Cnb (green) and the microtubule
692 marker UAS-mCherry::Jupiter (white), driven by the neuroblast-specific worGal4 transgene. Note that the
693 daughter centriole (Cnb^{+}) remains active and anchored to the apical cortex throughout interphase. The
694 second centrosome matures in prophase (00:39) after it reached the basal side of the cell. "00:00"
695 corresponds to telophase. Time scale is hh:mm and the scale bar is 3μm.

696

697 **Movie 2: Neuroblast expressing YFP::Cnb::PACT; related to figure S6.**

698 Larval neuroblast expressing YFP::Cnb::PACT (green) and the microtubule marker UAS-mCherry::Jupiter
699 (white), driven by the neuroblast-specific worGal4 transgene. Note that YFP::Cnb::PACT is present on
700 both centrioles. Both centrosomes remain active and anchored to the apical cortex throughout interphase.
701 Centrioles split in prophase (00:39) accompanied by a large spindle rotation (00:42 - 00:45), resulting in
702 normal asymmetric cell division. "00:00" corresponds to telophase. Time scale is hh:mm and the scale bar
703 is 3μm.

704

705 **Movie 3: Neuroblast expressing YFP::Cnb together with centriole tethered PACT::vhhGFP4;**
706 **related to figure S7.**

707 Larval neuroblast expressing the centriolar marker YFP::Cnb (green), the microtubule marker UAS-
708 mCherry::Jupiter (white) and the PACT::vhhGFP4 nanobody; both UAS lines are driven by the neuroblast-
709 specific worGal4 transgene. The PACT domain confines the nanobody predominantly to the mother
710 centriole. Both centrosomes remain active and anchored to the apical cortex throughout interphase.
711 Centrosome splitting occurs a few minutes before mitosis (00:36). "00:00" corresponds to telophase. Time
712 scale is hh:mm and the scale bar is 3μm.

713 **Movie 4: Neuroblast expressing Asl::GFP together with centriole tethered PACT::vhhGFP4; related**
714 **to figure S7.**
715 Larval neuroblast expressing the centriolar marker Asl::GFP (green), the microtubule marker UAS-
716 mCherry::Jupiter (white) and the PACT::vhhGFP4 nanobody; both UAS lines are driven by the neuroblast-
717 specific worGal4 transgene. Similar to the wild type control, the daughter centriole remains active and
718 anchored to the apical cortex throughout interphase. The mother centriole sheds its MTOC activity and
719 moves away in early interphase (00:15). At mitotic entry (00:45), the mother centriole matures after it
720 reached the basal side of the cell. "00:00" corresponds to telophase. Time scale is hh:mm and the scale bar
721 is 3μm.
722
723 **Movie 5: Wild type control neuroblast expressing Polo::EGFP; related to figure 5.**
724 Wild type control larval neuroblast expressing Polo::EGFP (green) engineered by CRISPR/Cas9
725 technology and the microtubule marker mCherry::Jupiter (white). Note that the daughter centriole remains
726 active and anchored to the apical cortex throughout interphase. The mother centriole matures at 00:42 after
727 it reached the basal cell cortex. "00:00" corresponds to telophase. Time scale is hh:mm and the scale bar is
728 3μm.
729
730 **Movie 6: Neuroblast expressing Polo::EGFP together with centriole tethered PACT::vhhGFP4;**
731 **related to figure 5.**
732 Larval neuroblast expressing Polo::EGFP (green) engineered by CRISPR/Cas9 technology, the microtubule
733 marker mCherry::Jupiter (white) and the PACT::vhhGFP4 nanobody; both UAS lines are driven by the
734 neuroblast-specific worGal4 transgene. Both MTOCs remain active and anchored to the apical cortex
735 throughout interphase. Centrioles split only 6 minutes before mitosis starts (00:36). The mitotic spindle
736 rotates significantly (00:42-00:48) to realign the spindle along the internal apical – basal polarity axis and

to ensure normal asymmetric cell division. “00:00” corresponds to telophase. Time scale is hh:mm and the scale bar is 3µm.

Movie 7: Neuroblast expressing GFP::Polo together with centriole tethered PACT::vhhGFP4; related to figure S7.

Larval neuroblast expressing the transgene GFP::Polo (green), the microtubule marker mCherry::Jupiter (white) and the PACT::vhhGFP4 nanobody; both UAS lines are driven by the neuroblast-specific worGal4 transgene. Both MTOCs remain active and anchored to the apical cortex throughout interphase. Centrioles split only 6 minutes before mitosis starts (00:48). “00:00” corresponds to telophase. Time scale is hh:mm and the scale bar is 3µm.